Active Site Structure and Mechanism of Human Glyoxalase I—An ab Initio Theoretical Study

Uwe Richter and Morris Krauss*

Contribution from the Center for Advanced Research in Biotechnology, National Institute of Standards and Technology, 9600 Gudelsky Drive, Rockville, Maryland 20850

Received March 5, 2001

Abstract: The structure of the active site of human glyoxalase I and the reaction mechanism of the enzyme-catalyzed conversion of the thiohemiacetal, formed from methylglyoxal and glutathione, to *S*-D-lactoylglutathione has been investigated by ab initio quantum chemical calculations. To realistically represent the environment of the reaction center, the effective fragment potential methodology has been employed, which allows systems of several hundred atoms to be described quantum mechanically. The methodology and the active site model have been validated by optimizing the structure of a known enzyme−inhibitor complex, which yielded structures in good agreement with the experiment. The same crystal structure has been used to obtain the quantum motif for the investigation of the glyoxalase I reaction. The results of our study confirm that the metal center of the active site zinc complex plays a direct catalytic role by binding the substrate and stabilizing the proposed enediolate reaction intermediate. In addition, our calculations yielded detailed information about the interactions of the substrate, the reaction intermediates, and the product with the active site of the enzyme and about the mechanism of the glyoxalase I reaction. The proton transfers of the reaction proceed via the two highly flexible residues Glu172 and Glu99. Information about the structural and energetic effect of the protein on the first-shell complex has been attained by comparison of the structures optimized in the local protein environment and in a vacuum. The environment of the zinc complex disturbs the C_s symmetry found for the complex in a vacuum, which suggests an explanation for the stereochemical behavior of glyoxalase I.

1. Introduction

The glyoxalase system, consisting of the two enzymes glyoxalase I (GlxI) and glyoxalase II (GlxII), is part of the glycolytic methylglyoxal pathway, which runs parallel to the ATP-generating glycolytic pathway.[1−3] It is presumably concerned with cell growth and cell division and starts with the conversion of dihydroxyacetone phosphate to methylglyoxal by methylglyoxal synthase. Several enzymatic reactions are then involved in the degradation of the cytotoxic methylglyoxal. On the most important route, the thiohemiacetal, formed nonenzymatically from methylglyoxal and glutathione, is converted by GlxI to *S*-D-lactoylglutathione, which is then hydrolyzed by GlxII to D-lactic acid and glutathione. Variation in the activity of the glyoxalase system may be related to diseases such as cancer and diabetes. It has been found that GlxI is highly activated in various cancer cells, while the activity of GlxII is reduced.[4,5] Under these conditions *S*-D-lactoylglutathione accumulates, which has been proposed to be tumor promoting. On the other hand, the highly reactive methylglyoxal inhibits the protein-synthesizing machinery of the cells and, thus, has a growth inhibitory effect.[1−3,6] Since the glyoxalase system represents the main factor in controlling the cell concentration of methylglyoxal, much effort has been devoted to searching for effective inhibitors of GlxI as a basis of a tumor-selective anticancer strategy.[7−14]

An essential prerequisite to the truly rational design of competitive inhibitors is detailed information about the active site structure and reaction mechanism. The structure of the human GlxI active site has been explored by various spectroscopic techniques[15−22] and X-ray crystallography.[23−25] It has been shown that the presence of one Zn^{2+} ion per active site is

(1) Mannervik, B.; Ridderström, M. *Biochem. Soc. Trans.* **1993**, *21*, 515−517. See also the following articles in the same issue.
(2) Thornalley, P. J. *Biochem. J.* **1990**, *269*, 1−11.
(3) Ray, M.; Ray, S. *Curr. Sci.* **1998**, *75*, 103−113.
(4) Jerzykowski, T.; Winter, R.; Matuszewski, W.; Piskorska, D. *Int. J. Biochem.* **1978**, *9*, 853−860.
(5) Ayoub, F.; Zaman, M.; Thornalley, P. J.; Masters, J. *Anticancer Res.* **1993**, *13*, 151−156.
(6) Lo, T. W. C.; Westwood, M. E.; McLellan, A. C.; Selwood, T.; Thornalley, P. J. *J. Biol. Chem.* **1994**, *51*, 32299−32305.
(7) Hamilton, D. S.; Creighton, D. J. *J. Biol. Chem.* **1992**, *35*, 24933−24936.
(8) Douglas, K. T.; Shinkai, S. *Angew. Chem., Int. Ed. Engl.* **1985**, *24*, 31−44.
(9) Lo, T. W. C.; Thornalley, P. J. *Biochem. Pharmacol.* **1992**, *44*, 2357−2363.
(10) Kavarana, M. J.; Kovaleva, E. G.; Creighton, D. J.; Wollman, M. B.; Eiseman, J. L. *J. Med. Chem.* **1999**, *42*, 221−228.
(11) Hamilton, D. S.; Kavarana, M. J.; Sharkey, E. M.; Eiseman, J. L.; Creighton, D. J. *J. Med. Chem.* **1999**, *42*, 1823−1827.
(12) Thornalley, P. J.; Ladan, M. J.; Ridgeway, S. J. S.; Kang, Y. *J. Med. Chem.* **1996**, *39*, 3409−3411.
(13) Murthy, N. S. R. K.; Bakeris, T.; Kavarana, M. J.; Hamilton, D. S.; Lan, Y.; Creighton, D. J. *J. Med. Chem.* **1994**, *37*, 2161−2166.
(14) Lo, T. W. C.; Thornalley, P. J. *J. Chem. Soc., Perkin Trans. 1* **1992**, *20*, 639−643.
(15) Hall, S. S.; Doweyko, A. M.; Jordan, F. *J. Am. Chem. Soc.* **1976**, *98*, 7460−7461.
(16) Sellin, S.; Eriksson, G.; Mannervik, B. *Biochemistry* **1982**, *21*, 4850−4857.
(17) Sellin, S.; Eriksson, G.; Aronsson, A.-C.; Mannervik, B. *J. Biol. Chem.* **1982**, *4*, 2091−2093.
(18) Rosevear, P. R.; Chari, R. V. J.; Kozarich, J. W.; Mannervik, B.; Mildvan, A. S. *J. Biol. Chem.* **1983**, *258*, 6823−6826.
(19) Sellin, S.; Eriksson, G.; Mannervik, B. *Biochemistry* **1987**, *26*, 6779−6784.
(20) Lan, Y.; Lu, T.; Lovett, P. S.; Creighton, D. J. *J. Biol. Chem.* **1995**, *270*, 12957−12960.

10.1021/ja0105966 CCC: $20.00
Published on Web 06/30/2001

essential for the activity of the native human enzyme. The metal ion is ligated by two glutamate residues, one glutamine residue, and one histidine residue. In addition, depending on whether an inhibitor or the product is bound to the active site, one or two water molecules might be coordinated to the zinc ion, which implies that the coordination behavior of the active site metal center is variable. The isomerization reaction has been proposed to proceed via a proton-transfer mechanism involving an enediolate intermediate and a base for the proton abstraction and transfer between the two corresponding carbon atoms.[15,22] The most recent crystal structure of human GlxI with the enediolate intermediate analogue HIPC-GSH bound in the active site[25] strongly suggests an "inner-sphere" mechanism, in which, for the *S*-stereoisomer of the thiohemiacetal, Glu172 acts as the proton-abstracting base, and the intermediate is stabilized by direct coordination to the metal center. In this crystal structure, Glu172 is not bound to the zinc complex. As a possible trigger or driving force for the removal of Glu172 from the zinc ion, the bifurcated H-bonding between the glutathionyl[glycyl] carboxyl group of the substrate and two peptidyl NH's in the main chain of the protein has been discussed.[26] These interactions also appear to stabilize a peptide loop over the active side, shielding the inhibitor from the bulk solvent. By means of the experimental results, Cameron et al.[25] deduced a qualitative reaction mechanism, in which the substrate enters the active site and coordinates to the zinc center, displacing water molecules and Glu172. Glu172 then abstracts the proton from C1, resulting in the formation of the zinc-bound enediolate intermediate. The proton is then transferred to C2, which causes the product to be formed and released from the active site. This mechanism was refined by Creighton and Hamilton in a recent minireview.[26] However, the possible role of active site residues other than Glu172, in particular that of Glu99, cannot been elucidated on the basis of the available experimental data. Furthermore, the structural and electronic changes of the substrate and active site complex during the process of substrate binding and the proton-transfer steps have not been determined.

A fundamental problem of the current experimental methods is that the structure of the native substrate bound in the active site cannot be accessed. For that reason, analogue structures are sought by modifying either the protein or the substrate. However, even small modifications change the local ionicity and the substrate binding in an essential way. The same problems arise when binding a molecule similar to a putative intermediate structure, commonly denoted as a transition state analogue, which is often electronically distinct from the intermediate of the actual reaction.

Quantum chemistry can supplement the experimental data with accurate structural details of the binding complexes of the substrate, intermediates, and products as well as of transition states. An accurate representation of the ionic hydrogen bonds, however, requires an ab initio quantum chemical treatment, which strongly limits the size of the systems feasible for calculation. A number of different approaches have been developed to resolve this problem, most of which combine quantum mechanical (QM) and molecular mechanical (MM) methods.[27] In these QM/MM methods, the relatively small reaction center is treated quantum mechanically, and the surrounding protein and the solvent are treated by a classical force field.

In this work, effective fragment potentials[28] (EFPs) have been used to represent the first shell of amino acid residues, the spectator region, surrounding the reaction center. The active region, which must contain all components directly involved in the actual chemical reaction, is treated by ab initio methods. The advantage of the EFP method over many common QM/MM methods is that the electronic properties of the environment are described basically at the same level as those of the active region. The EFPs are directly derived from ab initio calculations on single spectator fragments and contain the essential physics to represent the interaction of the active region with the surrounding protein. The main assumption made for the use of the EFPs is that the reaction center is shielded from the outside protein and solvent by the first shell of surrounding amino acid residues and that conformational changes beyond the spectator region do not affect the chemical reaction qualitatively. We further assume that the reaction occurs on a significantly shorter time scale than the changes of the average reaction field generated by the spectator region.

Using the EFPs, the structure of the active site of GlxI has been explored by quantum chemical calculations. The structure of the first-shell zinc complex has been optimized in a vacuum and in various EFP environments, giving insight into the effects of the protein and substrate on the complex structure. Minimum structures have been obtained for substrate/enzyme (**S**−**E**) and product/enzyme (**P**−**E**) complexes as well as for intermediate complexes of the GlxI reaction, which provides a detailed description of a reaction mechanism. Some aspects of the stereospecificity of the reaction are also discussed.

2. Methods

The EFP methodology has been described in detail elsewhere.[28,29] The EFPs account for the most important nonbonding interactions between the active and the spectator regions. All components of the EFPs are represented as linear expansions of Gaussian functions included as one-electron terms in the quantum mechanical Hamiltonian. An accurate representation of the electrostatic potential is achieved using a distributed multipolar analysis[30,31] (DMA) of the spectator charge distribution, multiplied by a distance-dependent screening function to account for charge penetration. The polarization of the spectator fragments by the electric field of the active part of the system is treated by a self-consistent perturbation model employing bond and lone-pair polarizabilities extracted from finite-field perturbation Hartree−Fock calculations on the separate models of the spectator fragments.[32] The electrostatic and polarization potentials were generated directly with the GAMESS-US program[33] package. The repulsive interactions are probed with a water molecule, and a grid of interaction energies is obtained in regions accessible for a water molecule to form hydrogen bonds. The exchange and charge-transfer contributions are derived by

(21) Garcia-Iniguez, L.; Powers, L.; Chance, B.; Sellin, S.; Mannervik, B.; Mildvan, A. S. *Biochemistry* **1984**, *23*, 685−689.
(22) Sellin, S.; Rosevear, P. R.; Mannervik, B.; Mildvan, A. S. *J. Biol. Chem.* **1982**, *257*, 10023−10029.
(23) Cameron, A. D.; Olin, B.; Ridderström, M.; Mannervik, B.; Jones, T. A. *EMBO J.* **1997**, *16*, 3386-3395.
(24) Ridderström, M.; Cameron, A. D.; Jones, T. A.; Mannervik, B. *J. Biol. Chem.* **1998**, *273*, 21623−21628.
(25) Cameron, A. D.; Ridderström, M.; Olin, B.; Kavarana, M. J.; Creighton, D. J.; Mannervik, B. *Biochemistry* **1999**, *38*, 13480−13490.
(26) Creighton, D. J.; Hamilton, D. S. *Arch. Biochem. Biophys.* **2001**, *387*, 1−10.
(27) Gao, J. In *Reviews in Computational Chemistry 7*; Lipkowitz, K. B., Boyd, D. B., Eds.; VCH: New York, 1995; pp 119−185.
(28) Day, P. N.; Jensen, J. H.; Gordon, M. S.; Webb, S. P.; Stevens, W. J.; Krauss, M.; Garmer, D.; Basch, H.; Cohen, D. *J. Chem. Phys.* **1996**, *105*, 1968−1986.
(29) Worthington, S. E.; Krauss, *Comput. Chem.* **2000**, *24*, 275−285.
(30) Stone, A. J. *Chem. Phys. Lett.* **1981**, *83*, 233−239.
(31) Stone, A.; Alderton, M. *Mol. Phys.* **1985**, *56*, 1047−1064.
(32) Garmer, D. R.; Stevens, W. J. *J. Phys. Chem.* **1989**, *93*, 8263−8270.
(33) Schmidt, M. W.; Baldridge, K. K.; Boatz, J. A.; Ebert, S. T.; Gordon, M. S.; Jensen, J. H.; Koseki, S.; Matsunaga, N.; Nguyen, K. A.; Su, S.; Windus, T. L.; Dupuis, M.; Montgomery, J. A., Jr. *J. Comput. Chem.* **1993**, *14*, 1347−1363.

means of a reduced variational space[34] (RVS) energy decomposition and are fitted to a linear combination of Gaussian functions.[35]

All geometry optimizations were performed at the RHF/4-31G SBK level of theory. This level of theory is sufficient to provide good qualitative insight into the interactions in the protein active site and the reaction. For a quantitative description of the energetics of the reaction, higher level approaches have to be employed.

For the generation of the EFPs, one polarization function was added to the non-hydrogen atoms. All calculations were performed using the GAMESS-US program. For all optimized structures, the standard RMSD threshold of 0.0001 was reached.

The active region of our active site model contains the glutathione conjugate and the first-shell zinc complex with His126, Gln33, Glu99, and Glu172 as well as one or two water molecules. Hydrogen atoms were added to the B-GSH/GlxI crystal structure[23] (B-GSH = *S*-benzylglutathione) using Molden.[36] The amino acid residues were capped with CH_3 at their Cα positions. The substrate was capped with CH_3 at the Cα atom of the cystyl residue of the tripeptide. The frozen spectator region for all EFP calculations of this study consists of the side chains of the residues Gln32, Leu160, Leu174, Leu69, Leu92, Met35, Phe162, Phe62, Phe67, Phe71, and Thr101 up to the Cα atoms (CH_3). These residues constitute the immediate surrounding of the substrate near the reaction center and are mostly part of the hydrophobic pocket that accommodates the S-substituent of the glutathione conjugate. Test calculations were performed, in which the glutathione conjugate was included completely. In these cases, the residues Arg122, Arg37, and Asn103, which interact with the glycyl residue of the tripeptide, were added as EFPs as well. However, the inclusion of these three residues and the full glutathione conjugate had no effect on the calculated structure of the B-GSH/GlxI complex but increased the computational costs considerably. Moreover, Arg122, Arg37, and Asn103 had to be excluded from the system, since these residues, when frozen at their positions in the B-GSH crystal structure, would keep the substrate from moving farther into the active site. The substrate, however, must move closer to the zinc center to be able to bind to the zinc complex. In the HIPC-GSH/GlxI crystal structure[25] (HIPC-GSH = *S*-(*N*-hydroxy-*N*-*p*-iodophenylcarbamoyl)glutathione), in which the inhibitor is bound to the zinc center, the Cα atom of the cystyl group of the glutathione conjugate is about 0.4 Å closer to the metal ion than in the B-GSH/GlxI complex. For these reasons, the smaller active site model described above was used throughout this study.

3. Results and Discussion

Definition and Validation of the Active Site Model. For the definition of the active site model, the crystal structure of the B-GSH/GlxI complex[23] was used. Concerning the reaction mechanism, this structure can be considered as the least significant of all available crystal structures for human GlxI. It was chosen to show that it is possible to calculate a reaction path, including substrate and product complexes and intermediate structures, starting from a crystal structure, which does not have a transition-state analogue or the product bound to the active site.

In the crystal structure of the B-GSH/GlxI complex, the active site zinc ion is coordinated by four protein residues (His126, Glu172, Glu99, Gln33) and one water molecule (W1). The coordination geometry is distorted square pyramidal with His126 as the axial ligand. ESR experiments on Co^{2+}-substituted GlxI[17] have indicated a distorted octahedral metal coordination. Proton relaxation studies on the Mn^{2+}-substituted enzyme[16] have shown two rapidly exchanging water molecules in the apo-enzyme, whereas only one water molecule could be detected when the inhibitor, *S*-(*p*-bromobenzyl) glutathione, or the product of the GlxI reaction, *S*-(D-lactoyl) glutathione, is bound in the active site. Apparently, the second active site water molecule (W2) is displaced in the B-GSH/enzyme complex as well.

Table 1. Optimized Structural Parameters for Various Active Site Model Systems

	Exp	EFP1	EFP2	EFP3	Tbp2	Sqp2[c]
			Bond (Å)			
Zn−E172	2.02	2.01	1.99	2.04	1.99	2.01
Zn−E99	1.99	1.99	1.99	2.01	1.98	2.00
Zn−Q33	2.02	2.15	2.09	2.15	2.11	2.04
Zn−H126	2.02	2.05	2.07	2.04	2.06	2.03
Zn−W1	2.11	2.17	2.23	2.11	2.30	2.22
			Angle (Deg)[a]			
E172−Zn−E99	154	144	147	155	119	154
Q33−Zn−W1	152	162	165	149	174	159
Q33−Zn−H126	102	104	107	104	91	108
H126−Zn−W1	106	94	90	101	86	92
			Dihedral Angle (Deg)[b]			
E172	74	67	67	102	88	109
E99	−176	168	166	168	124	−125
Q33	164	147	150	152	166	180

[a] Angles between atoms directly bonded to Zn. [b] Angles between planes of CD−OE1−Zn and OE1−Zn−NE2(H126). [c] Cα atoms of H126 and Q33 frozen.

The reaction center of GlxI was modeled with the inhibitor B-GSH bound to the active site. In the first set of calculations, the positions of the Cα atoms of the four ligand residues were frozen. The inhibitor was either represented as EFP within the spectator region (**EFP1**) or included in the all-electron part of the quantum system with its coordinates kept fixed (**EFP2**). Both approaches yield almost identical results for the structure of the zinc complex (Table 1), which demonstrates that the accuracy of the EFP methodology can be comparable to that of the full ab initio treatment. Differences were found mainly in the orientation of the carboxyl groups and the Zn−W1 distance. These changes should mostly result from the fact that the EFP for the inhibitor was generated with a polarized basis set, whereas the basis set used for the all-electron system does not contain polarization functions. It will be shown that the orientation of the carboxyl groups and the Zn−W1 distance are very sensitive to changes of the surrounding potential.

Both **EFP1** and **EFP2** reproduce the experimental structure reasonably well (Figure 1). They show a distorted square pyramidal coordination geometry, although a tendency toward a trigonal bipyramidal coordination with Gln33 and W1 as the axial ligands can be recognized. The bond lengths from the two glutamate residues to the zinc ion agree very well with the experimental values, while the other calculated Zn−ligand distances are somewhat longer than in the X-ray structure. This might be a consequence of the distortion of the complex away from a square pyramidal to a more trigonal bipyramidal structure, resulting in a decrease in the angles between the axial ligands and His126. From the computational point of view, factors such as electron correlation and deficiencies in the used one-electron basis as well as the constraints imposed on the Cα positions constitute sources of error. However, we note that the experimental values depend on the initial parameters used in the structure refinement, which might not always be appropriate for the special situation in a certain protein. Thus, protein crystal structures are often not accurate enough to give insight into the electronic peculiarities. For example, all the C−O distances of Glu172 and Glu99 in the crystal structures of GlxI are of almost identical length, which is electronically impossible. The bond lengths must be different, since one of the oxygen atoms of each glutamate residue binds to the zinc

(34) Stevens, W. J.; Fink, W. *Chem. Phys. Lett.* **1987**, *139*, 15−22.
(35) Stevens, W. J. Utility programs for determining repulsive EFP and screening functions, 1996.
(36) Schaftenaar, G.; Noordik, J. H. *J. Comput.-Aided Mol. Des.* **2000**, *14*, 123−134.

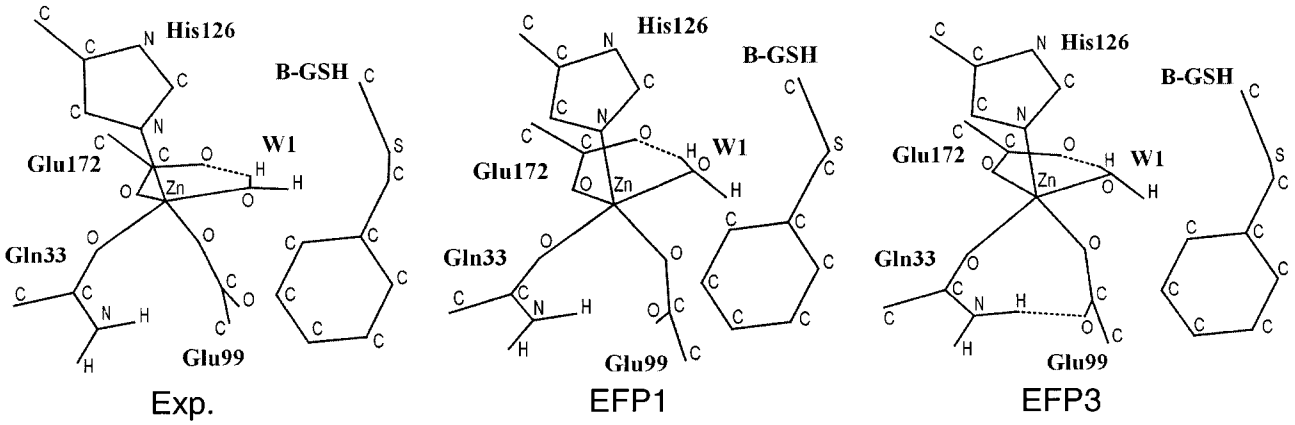

Figure 1. Optimized active site structure of the B-GSH complex with frozen (**EFP1**) and unfrozen (**EFP3**) glutamate Cα positions compared to the crystal structure (**Exp**).

ion, resulting in a C−O single bond that has to be notably longer than the remaining C−O double bond for the non-Zn-bonded oxygen atom. In fact, in some cases this trend is even reversed in the crystal structure.

Removing the constraints on the glutamate Cα atoms and reoptimizing the complex (**EFP3**) leads to a significant improvement with respect to the experimental Zn−water distance and the bond angles (see Table 1). The Cα atoms of Glu99 and Glu172 move 1.4 and 0.8 Å from their original positions, respectively. This allows the carboxylate group of Glu99 to turn toward Gln33 so that a hydrogen bond is formed between these two residues. The effect of releasing the two Cα atoms on the energy (∼8 kcal mol^{-1}) is rather small and is likely due to the formation of the additional hydrogen bond. The stabilization energy becomes even smaller (∼5 kcal mol^{-1}) if no substrate or inhibitor is present. An attraction between Glu99 and Gln33 can be seen in **EFP1** and **EFP2** as well. On the other hand, the crystal structure of the B-GSH/GlxI active site shows no indication of such an interaction. The change in the orientation of Glu99 can be considered the most striking difference between the calculated and experimental results. It suggests the presence of one or more unresolved solvent water molecules in the crystal structure.

The calculations for the B-GSH/GlxI complex show that structural parameters of the enzyme active site in good agreement with the experiment may be obtained using the EFP methodology. Moreover, they reveal information about interactions in the active site that is difficult to discern from the crystal structure. Given the good agreement demonstrated above, it is believed that, by employing the EFPs to represent the environment of the reaction center and using an appropriate model for the thiohemiacetal, detailed structural and mechanistic information for the GlxI reaction can be obtained.

Reaction Path Structures. The thiohemiacetal model was constructed in the active site beginning with the Cα atom of the cystyl group of the glutathione conjugate located at its position in the B-GSH/GlxI complex. Only the *S*-enantiomer of the substrate was considered, although the enzyme metabolizes both the *S*- and *R*-forms and converts them to *S*-D-lactoylglutathione.[37−39] A number of different initial conformations for the substrate in the active site were optimized with the aim to find a productive **S**−**E** complex, which we define as a **S**−**E** arrangement, from which the chemical reaction can be initiated. As discussed in detail below, for GlxI, the intitial step corresponds to the abstraction of the proton from the carbon atom of the *S*-substituent directly bound to the sulfur atom (C1). Most of the trial conformations yielded complexes for which a proton abstraction was not possible, including all systems with zinc-bound water molecules. It was concluded that, for an "inner-sphere" mechanism, the water molecules have to be displaced from the complex while the substrate moves into the active site prior to the actual reaction. "Outer-sphere" mechanisms, in which a zinc-bound water molecule or hydroxyl ion is involved in the reaction, have been discussed in the literature as well. Such mechanisms are not considered in this paper. We believe, however, that the available experimental data, in particular the crystal structure with the enediolate intermediate analogue bound to the zinc center, provide strong evidence for an "inner-sphere" mechanism for glyoxalase I.

Reactive S−E Complex (A). After the water molecules were removed from the active region, various **S**−**E** complexes were obtained, in which either one or both oxygen atoms of the substrate are directly bound to the zinc center. For these complexes, the proton abstraction from C1 by Glu172 and the abstraction of the hydroxyl proton by Glu99 as possible initial reaction steps were investigated. This was done by moving the protons from C1 to Glu172 and from the hydroxyl group to Glu99, respectively, followed by a reoptimization of the complex. Somewhat surprisingly, only one of the calculated **S**−**E** complexes turned out to be productive, and the proton transfer between C1 and Glu172 was not reversed during the optimization. In all other calculations the particular proton moved back to its initial position at the substrate, either from Glu172 to C1 or from Glu99 to the hydroxyl oxygen (O1).

The structure of the calculated productive complex (**A**) is shown in Figure 2, and the most important structural parameters are summarized in Table 2. The optimization was started from an initial structure with no binding interactions between the substrate and the zinc complex. The hydroxyl and the carboxyl group of the substrate were in a conformation that would yield the cis conformer upon abstraction of the C1 proton (H1). The initial Zn−O distances for the hydroxyl (O1) and carboxyl (O2) oxygen atoms were 4.32 and 5.50 Å, respectively. During the optimization the substrate moved farther into the active site, which was not possible while one or two water molecules were bound to the complex. Hydrogen bonds were formed between the substrate hydroxyl group and Glu99 and between the carboxyl group and Gln33. These interactions then helped to bring both substrate oxygen atoms into coordination range to

(37) Griffis, C. E. F.; Ong, L. H.; Buettner, L.; Creighton, D. J. *Biochemistry* **1983**, *22*, 2945−2951.
(38) Rae, C.; O'Donoghue, S. I.; Bubb, W. A.; Kuchel, P. W. *Biochemistry* **1994**, *33*, 3548−3559.
(39) Landro, J. A.; Brush, E. J.; Kozarich, J. W. *Biochemistry* **1992**, *31*, 6069−6077.

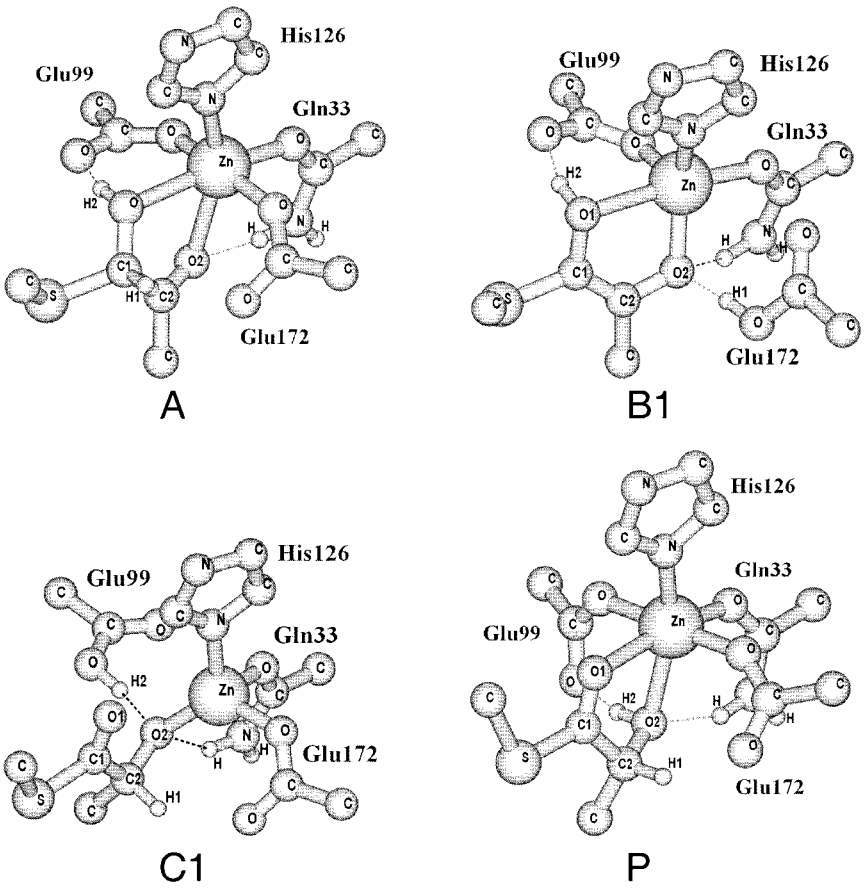

Figure 2. Calculated structures of the substrate/enzyme, product/enzyme, and intermediate complexes of the glyoxalase I reaction.

Table 2. Important Bond Lengths (Å) for the Calculated Reaction Path Structures

	A	B1	B2	C1	C2	P
			Glu172			
Zn−Oϵ1	1.99	3.49	2.21	1.95	1.96	1.99
Oϵ1−Cγ	1.29	1.23	1.23	1.30	1.29	1.30
Oϵ2−Cγ	1.26	1.34	1.34	1.25	1.26	1.26
Oϵ2−H1	2.23	1.01	0.98	2.31	2.26	2.10
			Glu99			
Zn−Oϵ1	2.04	2.00	2.01	4.13	2.28	2.09
Oϵ1−Cγ	1.28	1.29	1.28	1.23	1.23	1.28
Oϵ2−Cγ	1.28	1.27	1.28	1.35	1.35	1.28
Oϵ2−H2	1.52	1.61	1.58	1.02	0.98	1.50
			His126			
Zn−N	2.08	2.03	2.11	2.04	2.12	2.08
			Gln33			
Zn−Oϵ1	2.06	2.04	2.06	2.01	2.04	2.08
Oϵ1−Cγ	1.26	1.26	1.27	1.27	1.26	1.26
Nϵ2−Cγ	1.34	1.34	1.34	1.34	1.34	1.34
H(N)−O2	2.01	2.16	1.83	2.06	1.83	2.01
			Substrate			
Zn−O1	2.42	2.47	2.47	3.02	2.86	2.37
Zn−O2	2.45	1.97	2.04	1.96	1.99	2.35
C1−C2	1.54	1.36	1.37	1.54	1.55	1.54
C1−O1	1.42	1.41	1.42	1.23	1.24	1.23
C1−H1	1.09	3.48	2.32			
C2−H1		2.49	2.25	1.10	1.09	1.09
C2−O2	1.24	1.37	1.35	1.42	1.40	1.44
O1−H2	1.02	1.00	1.00		1.76	

the metal cation. In the optimized structure Glu172 is in a position to abstract H1 from the activated C1 with an O−H1 distance of 2.23 Å. The general complex structure can be considered as distorted octahedral. However, the coordination of the substrate to the metal is very weak for both O1 and O2, while the Zn−ligand bonds are still short due to strong binding. There is no significant charge redistribution within the substrate and the zinc complex compared to the separated entities. Only the Zn−OE2(Glu99) bond is slightly elongated as the result of the H-bonding to the substrate hydroxyl group, which reduces the effective negative charge and the electron donor capability of the glutamate residue to the metal ion.

First Intermediate Complex (B). As described above, the only possible step from **A** in the GlxI reaction is the proton abstraction from C1 by Glu172. The structure of the complex after abstraction of H1 by Glu172 was optimized both with the positions of the Cα atoms of the two glutamate ligands unfrozen (**B1**) and frozen (**B2**). In the unfrozen case (see Figure 2), the protonated Glu172 has dissociated completely from the zinc ion. The abstraction of the proton results in an electron redistribution in the substrate, which leads to the proposed enediolate intermediate with a C1−C2 double bond (Table 2). O2 now strongly binds to the metal ion, whereas the hydroxyl group remains only slightly zinc coordinated, but strongly hydrogen-bonded to Glu99.

The calculated structure **B1** is similar to the crystal structure of the HIPC-GSH/GlxI complex,[25] especially with respect to the orientation of the substrate in the active site. The resemblance becomes even closer when the hydroxyl proton (H2) is removed from the model system and the structure is reoptimized (Figure 3, Table 3). The removal of H2 from the quantum system causes H1 to move from Glu172 to O2, since only two negatively charged ligands are accepted by the metal dication. As in the HIPC-GSH/GlxI complex, the modified substrate then binds more strongly to the metal ion with both oxygen atoms. We assume that Glu172 in the HIPC-GSH/GlxI complex is protonated as well, whereas the inhibitor must be negatively

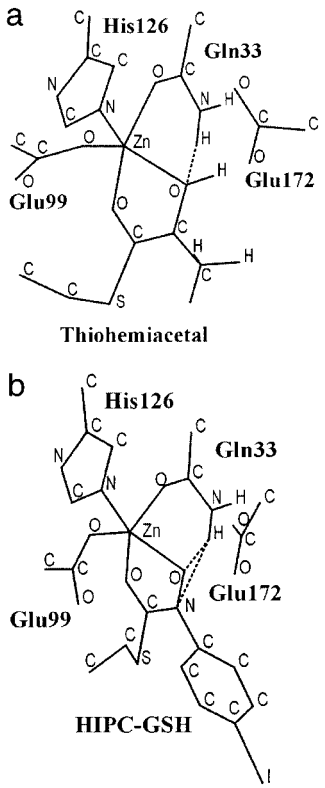

Figure 3. Reoptimized structure of the substrate/enzyme complex after the removal of H2 (a) compared with the crystal structure of the HIPC-GSH/GlxI complex (b).

Table 3. Bond Lengths (Å) of the Reoptimized Structure of the **S**−**E** Complex after the Removal of H2 (A(−H2)) Compared with the Crystal Structure of the HIPC-GSH/GlxI Complex

bond	HIPC-GSH/GlxI	A(−H2)
Zn−Glu99	1.89	1.99
Zn−His126	2.10	2.06
Zn−Gln33	1.99	2.14
Zn−O1	2.14	2.06
Zn−O2	2.09	2.14
C1−C2/N	1.34	1.36
C1−O1	1.23	1.34
C2/N−O2	1.30	1.43

charged, since otherwise, the enediolate intermediate analogue would not bind as strongly to the metal center as it is seen in the crystal structure. In this way, the charge balance of the zinc complex is retained. These considerations imply that the long-range effect of the H-bonding between the glutathionyl[glycyl] carboxyl group of the substrate and two peptidyl NH's in the main chain of the protein might not be the main force to drive Glu172 away from the zinc ion. In contrast to the proposed mechanisms, our results suggest a concerted process for the first reaction step of substrate binding to the zinc ion, proton abstraction from C1 by Glu172, and dissociation of Glu172 from the metal. In this process, which might involve a cyclic transition state as discussed by Creighton and Hamilton,[26] the negative charge of Glu172 is transferred to the substrate. Therefore, the substrate is able to bind strongly to the zinc center while the neutral Glu172 is released from the metal ion. In this process, again, the charge balance of the complex is retained.

It should be noted that the calculated structures discussed above are a further justification of our approach to investigate the enzyme active site and determine the reaction mechanism. They show that the structure of the B-GSH/GlxI complex can be leveraged into a structure very similar to the HIPC-GSH/GlxI complex by modeling a molecule electronically similar to the inhibitor HIPC-GSH into the active site. Therefore, we assume that we can also leverage the active site structure of the **S**−**E**, **P**−**E**, and intermediate complexes in the same manner, provided that the glutathione binding site does not change significantly.

Scheme 1

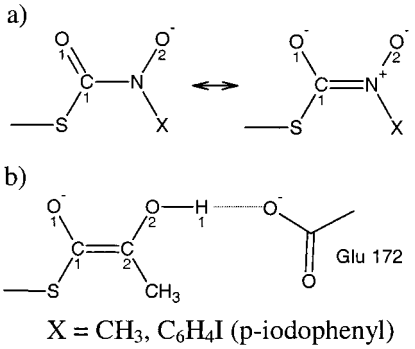

X = CH_3, C_6H_4I (p-iodophenyl)

The binding of the HIPC-GSH inhibitor and the enediolate anion to the metal ion can be understood by means of the valence bond (VB) structures shown in Scheme 1. For the inhibitor HIPC-GSH, the binding can be described by two resonance structures (see Scheme 1a). O2 is negatively charged in both structures, whereas O1 is negatively charged only in one. Therefore, O2 is bound more tightly to the zinc ion than O1, resulting in a slightly shorter Zn−O bond distance for the former (2.09 vs 2.13 Å) in the crystal structure.

For the endiolate dianion, only one appropriate VB structure (Scheme 1b) can be drawn, in which O1 possesses the negative charge and O2 is protonated. Consequently, Zn−O1 is somewhat shorter than Zn−O2. The fact that the Zn−O2 bond is still short is due to the strong hydrogen-bonding of the proton to Glu172, which considerably weakens the O2−H bond.

Freezing the glutamate Cα positions (**B2**, see Table 2) prevents Glu172 from leaving the Zn ion completely after abstracting the proton, although the corresponding Zn−O distance is significantly larger compared to that in **A**. As a further result, O2 does not bind as strongly to the metal ion as in **B1**. The distance from the abstracted proton to C2 is only 2.25 Å, and the charge distribution in **B2** is more favorable for delivering the proton to C2 than in **B1**, since, according to the Mulliken population analysis, C2 is less positively charged in **B2** (−0.02 vs +0.17). This implies that Glu172 does not need to leave the Zn ion completely after the proton abstraction. We suppose that the structure in the real protein is somewhere between **B1** and **B2**, depending on the flexibility the protein backbone. The temperature factors for the Cα atoms of the zinc ligands in the HIPC-GSH/GlxI crystal structure indicate that the protein is rather rigid at these positions. Thus, the energy gained by moving the protonated Glu172 away from the zinc center in our model system may well be compensated by the energy required for moving the backbone in the protein. In our calculations, **B1** is energetically 4.8 kcal mol^{-1} higher than **A**. The energy penalty due to the freezing of the glutamate Cα positions (**B2**) is 13.3 kcal mol^{-1}.

Second Intermediate Complex (C). Assuming that no water molecule is involved, the next reaction step could be either the abstraction of H2 by Glu99 or the immediate transfer of H1 from Glu172 to C2. The calculations for this step were initiated from **B2**, since in **B1** Glu172 had moved too far away from the reaction center. Again, structures were calculated for frozen and unfrozen glutamate Cα positions. It turned out that there is no

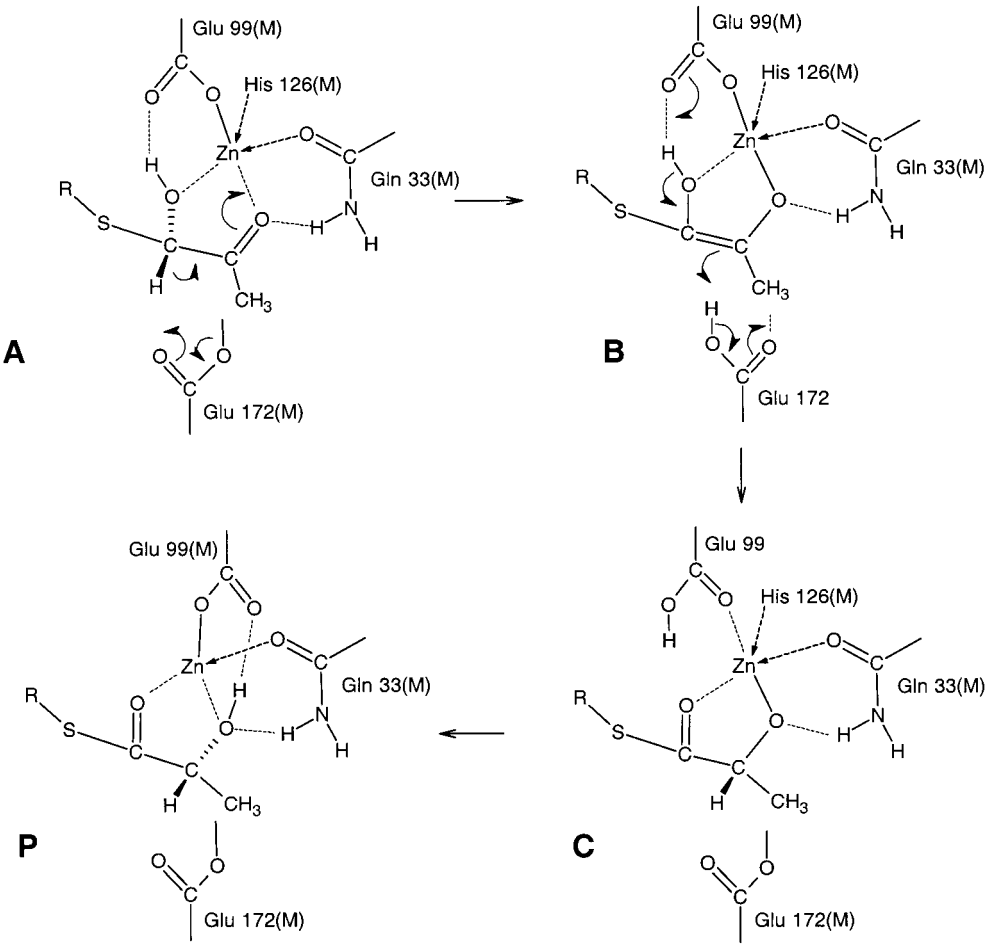

Figure 4. Schematic reaction path for the glyoxalase I reaction. For clarity, His126 is not shown in **P**. (M) means that the residue is strongly coordinated to the zinc ion.

stable structure in which, with respect to **B2**, only H2 is transferred from O1 to Glu99. The optimized structure returns to structure **B2**, even if the protonated Glu99 was turned out of hydrogen-bonding range to O1.

The proton transfer from Glu172 to C2, however, results in the formation of a C1−O1 double bond, which drives the transfer of H2 to Glu99. O1 coordinates only very weakly to the zinc ion. Glu172 is strongly bound to the metal again, whereas, in the unfrozen case (**C1**), the protonated Glu99 has left the zinc center. Keeping the Cα positions fixed (**C2**, see Table 2) prevents Glu99 from moving out of the zinc coordination range, but the Zn−O distance is elongated by about 0.27 Å compared to that in **B2**. The energy of **C2** is 21.6 kcal mol^{-1} higher than that of **C1**, which may be regarded in the same manner as the energy difference between **B1** and **B2**. **C2** is about 1.1 kcal mol^{-1} lower in energy than **B2**.

Product Complex (P). From **C**, there are two different pathways possible to yield a **P**−**E** complex. The first is the direct transfer of H2 to O2 via Glu99. This pathway is supported by the fact that, upon geometry optimization, the proton moves to O2 with no energetic barrier, if the calculation is started with the protonated Glu99 turned somewhat toward the carboxyl group and out of hydrogen-bonding range of O1. In the resulting structure (**P**), both substrate oxygen atoms only slightly coordinate to the zinc ion with calculated bond orders less than 0.05. The two glutamate residues bind strongly to the metal center as in **A**. The calculated energies for **A** and **P** are within 1 kcal mol^{-1}. The binding potential of *S*-D-lactoylglutathione to the metal ion appears to be very shallow. Depending on the starting conformation, a number of slightly different **P**−**E** complexes with varying Zn−O distances were obtained, with energies very close to that of **P**.

The second pathway to yield the *S*-D-lactoylglutathione is the protonation of O2, e.g., by a nearby water molecule. As in **P**, the product is only very weakly coordinated to the zinc ion with both oxygen atoms. Glu99 and Gln33 are hydrogen-bonded to O1 and O2, respectively. However, for a water molecule to be able to protonate O2, it has to be activated. Considering the active site structure, there is no obvious way to achieve this. Furthermore, there is no possibility for the resulting hydroxide anion to recover a proton easily. Therefore, it would certainly attack the zinc ion, while Glu99 would not move back to bind to the metal. A through-water proton transfer from Glu99 to O2 seems to be unlikely as well, since the water molecule does not fit between Glu99 and O2 in a manner that enhances proton tunneling. The same arguments hold for the structures **A** and **B**, for each of which, in principle, the protonation of O2 as next step is conceivable. Hence, our results strongly favor a glyoxalase I reaction without direct involvement of water molecules, although we cannot exclude their participation completely on the basis of our results.

Reaction Path (Figure 4).[40] A proton-transfer mechanism via an enediol intermediate has been generally accepted for the GlxI reaction. Moreover, the recently determined crystal struc-

(40) The mechanism shown in Figure 4 bears great similarities, including the transfer of H2 between the substrate oxygen atoms by Glu99, to the one proposed by Creighton and Hamilton in their recent minireview (see ref 26), which was published after the submission of our paper.

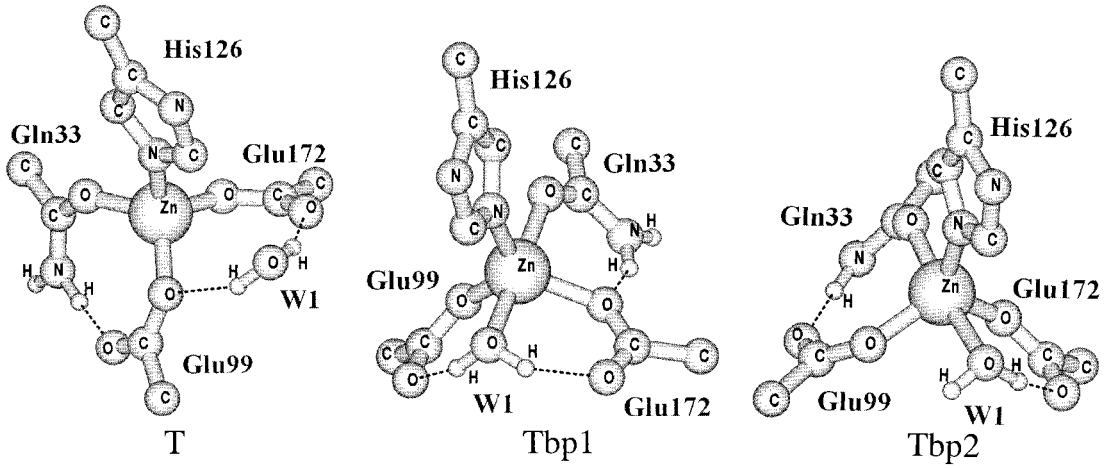

Figure 5. Optimized vacuum structures of the first-shell zinc complex.

ture of human GlxI with the enediol/transition-state analogue HIPC-GSH bound to the active site strongly suggests that the zinc ion of the native enzyme plays a direct catalytic role in the isomerization reaction. Our results support these facts, and the reaction path which can be realized on the basis of the calculated structures and bond orders agrees with that proposed by Cameron et al.[25] and Creighton and Hamilton[26] on many points. It should be stressed again that we cannot provide information about changes in the global protein structure while the substrate moves in to and out of the active site, and that we have no information about structural changes outside the first coordination shell during the reaction. Our approach is based on the assumption that, in the time scale of the actual chemical reaction, the structure of the surrounding of the reaction center and, thus, its electrostatic environment remain essentially unchanged. The reaction mechanism we are able to describe starts when the substrate has entered the active site and is locked there by hydrogen-bonding of the glycyl and glutamyl residues of the tripeptide to the protein. While moving into the active site, the substrate displaces the weakly bound water molecules from the zinc ion. Presumably, the water molecules stay in the vicinity of the reaction center and hydrogen-bond to the polar zinc ligands. They might support product release or assist in the transfer of protons. As mentioned previously, our calculations do not support direct involvement of water molecules in the proton-transfer processes of the conversion of the thiohemiacetal to *S*-D-lactoylglutathione.

When the substrate is locked in the active site and the *S*-substituent of the glutathione is in a conformation suitable to form a productive **S**−**E** complex, it is pulled further into the active site, forming hydrogen bonds to Glu99 and Gln33. In the productive **S**−**E** complex found in this study, both substrate oxygen atoms are weakly coordinated to the metal (**A**, see Figures 2 and 4). In the first step of the reaction, Glu172 abstracts the proton from C1. A *cis*-enediolate intermediate is formed with the negative charge at O2, which strongly binds to the zinc ion (**B**). Concurrently, the protonated residue moves away from the metal center. It is not clear whether Glu172 leaves the metal center completely. This depends on the flexibility of the corresponding part of the protein backbone. Assuming that Glu172 remains close to the zinc ion, the position of Glu172 is very well suited to deliver the proton directly to the C2 atom of the substrate without further intermediate steps. The protonation of C2 results in an electron redistribution in the substrate that causes the hydroxyl proton H2 to move to Glu99. This residue, in the protonated form, then leaves the metal center, while Glu172 returns and binds to the zinc (**C**). In the final step, Glu99 delivers the proton to O2, thereby forming a strong coordination to the metal ion (**P**). The resulting product *S*-D-lactoylglutathione is only very weakly coordinated to the zinc center and can easily leave the active site, which closes the catalytic cycle.

It should be mentioned that O2 remains hydrogen-bonded to Gln33 throughout all the described reaction steps. This fact might be targeted in the design of new GlxI inhibitors.

Effects of the Protein on the Active Site Zinc Complex. To gain more insight into the energetic and structural effects of the protein on the first-shell zinc complex as well as the stereospecificity of the glyoalase I reaction, further calculations were performed for the complex in a vacuum and the EFP field. Thereby the number of water molecules was varied and various constraints were imposed on the quantum system during the geometry optimizations. All vacuum structures were obtained for a minimal model system (CH_3COO^- (acetate) for Glu, CH_3-$CONH_2$ (acetamide) for Gln, and imidazol for His) as well as for a complex including all ligands up to their Cα atoms.

Unconstrained optimization shows that the lowest energy structure of the first-shell zinc complex in a vacuum is tetrahedral (Figure 5, **T**) if only one water molecule is present. During the optimization, the water molecule (W1) is repelled from the metal center and remains hydrogen-bonded to the OE1 atom of Glu99 and the OE2 atom of Glu172, thus shielding the two glutamate residues from each other. A similar result was found by Ventura and Cubas[41] in their semiempirical calculations. Another hydrogen bond is formed between the OE2 atom of Glu99 and the amino group of Gln33. Two other low-lying minimum structures for the vacuum complex were localized, both exhibiting trigonal bipyramidal coordination geometry with the water molecule and Glu33 as the axial ligands. In both structures, W1 hydrogen bonds to the OE2 atom of Glu172, while the OE2 atom of Glu99 binds either to W1 (**Tbp1**) or to Gln33 (**Tbp2**). Concerning the hydrogen-bonding pattern, the orientation of the ligand functional groups, and the binding parameters in general, **Tbp2** closely resembles the vacuum structure obtained with the Cα positions of the ligands kept frozen at their original positions. It is also very similar to the structure optimized in the field of the surrounding protein represented by EFPs including the B-GSH inhibitor (see Table 1).

(41) Ventura, O. N.; Cubas, M. L. *Int. J. Quantum Chem.* **1992**, *44*, 699−722.

Calculations with the Cα atoms of His126 and Gln33 kept frozen at the experimental position reveal a remarkable flexibility of the two glutamate residues, which is needed for the proton-transfer steps of the GlxI reaction. The change in energy, compared to the system with all four Cα atoms constrained, is small (2−5 kcal mol^{-1}), although, depending on the environment (vacuum, first-shell residues, inhibitor), the glutamate Cα positions may differ considerably from the B-GSH crystal structure. Moreover, the orientation of the glutamate carboxyl groups changes significantly with the environment, both with and without constraints on the Cα positions.

The Cα positions and the orientation of His126 and Gln33 in different environments change only very slightly upon removing the geometrical constraints, suggesting a rather inflexible arrangement of these two ligands. Apparently, in GlxI, His126 and Gln33 are in optimal positions to accommodate the zinc ion and form the first-shell complex. We suppose that the zinc ion would not bind at all if the complex were forced into an energetically unfavorable structure by the protein.

A similar set of calculations for the first-shell zinc complex was carried out with two water molecules (W1 and W2), again starting from the structure experimentally found for the B-GSH/GlxI system. W2 was positioned at the sixth coordination site at a Zn−O distance of about 2.1 Å. Since there are different ways to initially orient W2, a number of different hydrogen-bonding patterns are possible. We do not intend to discuss all calculated structures in detail here. In most structures the complex has a trigonal bipyramidal coordination geometry with either the two glutamate residues or W1 and Gln33 as axial ligands. In none of the optimized structures is W2 directly bound to the zinc ion, and neither Glu99 nor Glu172 is ever directly H-bonded to Gln33 (Zn−W2 = 3.2−3.6 Å). The second water molecule assists W1 in shielding the two glutamate residues from each other by hydrogen-bonding either to one of the two glutamate residues and Gln33 or to all three ligands. As for the single water system, the bond distance from W1 to the metal center varies significantly among the different structures. This bond distance seems to be determined mainly by the orientation of the glutamate residues and the overall hydrogen-bonding pattern in the complex. The Zn−W1 distance is optimal in the sense that it shields the two glutamate residues from each other most effectively. The direct binding of the water molecule to the zinc center should generally be weak. We obtained binding energies of 10−15 kcal mol^{-1} for W1 and W2. However, at the HF/4-31G level the binding energy is greatly overestimated, which is attributed to a large basis set superposition error (BSSE). But even if one corrects for the BSSE, the calculated value would not reflect the binding energy of the water molecules to the zinc ion, but it would also include the hydrogen-bonding to the glutamate residues. The latter might even contribute more to the calculated binding energy than the direct zinc−water coordination. This suggests that when the substrate enters the active site of GlxI, the zinc-coordinated water molecules are easily displaced.

Two interesting structures for the two-water complex are shown in Figure 6. The complex was optimized in a vacuum as well as in the field of the surrounding protein with the Cα atoms of His126 and Gln33 kept frozen. In a vacuum (**Sqp1**), the complex has almost perfect C_s symmetry, which is only slightly perturbed by the side chain of Gln33. W1 and W2 are hydrogen-bonded to both glutamate residues. W2 additionally hydrogen bonds to Gln33. In the complex embedded in the protein environment (**Sqp2**), W2 is hydrogen-bonded to Glu172, Glu99, and Gln33, while W1 hydrogen-bonds to Glu172 only,

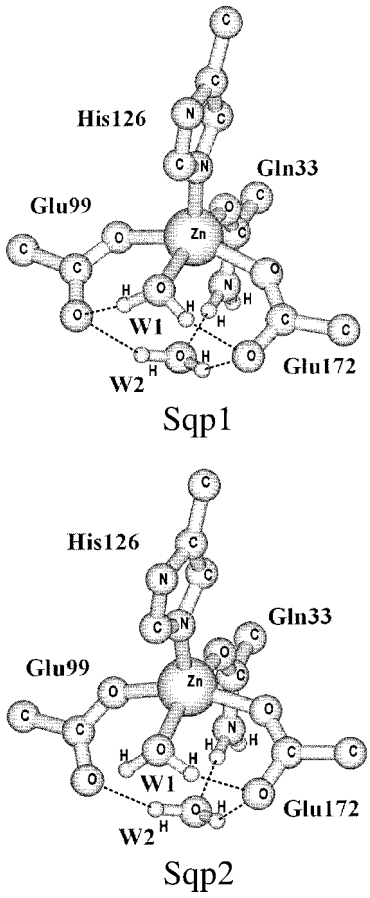

Figure 6. First-shell zinc complex with two water molecules. **Sqp1**, unconstrained vacuum structure; **Sqp2**, structure in the EFP field with Cα atoms of His126 and Gln33 frozen.

although the distance from W1 to the OE2 atom of Glu99 (O−H = 2.05 Å) is also close to hydrogen-bonding distance. Thus, the "symmetry" of the complex is slightly distorted by the protein environment, which could be the key factor for the stereospecific formation of *S*-D-lactoylglutathione from both the *S*- and *R*-diastereomers of the thiohemiacetal. Since W2 is out of the coordination range to the zinc ion (Zn−W2 = 3.55 Å), the coordination geometry of the complex should clearly be considered as square pyramidal in both cases. In fact, except for the orientation of the glutamate carboxylate functions and the Zn−W1 distance, the **Sqp2** structure is very similar to the experimental structure of the B-GSH/GlxI complex (see Table 1), supporting our assumption of a missing water molecule in the crystal structure. Removing W2 from the quantum systems and reoptimizing again yields trigonal bipyramidal complexes. Apparently, the nature of the molecule entering the active site of GlxI and approaching the complex on its sixth coordination site has a substantial effect on the complex structure, considering both the general coordination geometry and the orientation of the glutamate carboxyl functions.

Stereospecificity of the Reaction. The stereochemical behavior of glyoxalase I is still a matter of great controversy. Apparently, the enzyme indiscriminately metabolizes both diastereomers of the methylglyoxal thiohemiacetal, the *S*- and the *R*-forms, with no detectable difference in the reaction rate. Various mechanisms for the transformation of both diasteromers to *S*-D-lactoylglutathione have been discussed on the basis of NMR studies and other experimental findings.[26,37−39] For structural reasons, Creighton and Hamilton favor a "dissociative" pathway,[26] in which the enzyme catalyzes the interconversion

of the substrate diastereomers prior to converting the *S*-diastereomer to the product. Most other proposed mechanisms involve significant structural changes in the active site and, therefore, should be very unlikely.

Our calculations do not support a "dissociative" mechanism. One reason for this is that the abstraction of the hydroxyl proton by Glu99, which, according to the mechanism developed by Creighton and Hamilton, triggers the expulsion of the glutathionyl mercaptide anion from the thiohemiacetal function of the substrate, turned out to be not possible, as discussed earlier in this paper. We assume that even if this step was possible, it would cause the hydroxyl oxygen (O1) to bind strongly to the zinc ion, and, concomitantly, Glu99 would dissociate from the metal zinc ion. The expulsion of the mercaptide ion, on the other hand, would not conserve the charge of the zinc complex.

Our results suggest that the *S*- and *R*-forms of the substrate are converted via slightly different reaction mechanisms. From the *R*-diasteromer H1 cannot be abstracted by Glu172. The abstracting base for H1 must be Glu99. However, Glu99 cannot deliver the proton to C2, since this would yield *S*-L-lactoylglutathione as the product. Assuming again that no water molecule is directly involved in the reaction, Glu172 receives H2 and transfers it, as for the *S*-thiohemiacetal, to C2, whereas H1 goes to O2. Thus, the order of the reaction steps differs for the two stereoisomers, which, for methylglyoxal as the substrate, obviously does not appreciably affect the overall energetics and the rate of the reaction.

Considering the structure of the active site and the fact that abstraction of H1 from C1 is the critical factor in the GlxI reaction, it is not surprising that GlxI consumes both stereoisomers of the methylglyoxal thiohemiacetal. The arrangement of the zinc ligands is more or less symmetric (C_s), and, despite the different hydrogen-bonding pattern in the crystal structures, Glu99 and Glu172 are almost equivalent and both well suited to abstract H1 from the *R*- and *S*-thiohemiacetal, respectively. The more challenging question is why only *S*-D-lactoylglutathione is formed. We suppose that, if the active site were perfectly symmetric like the vacuum two-water complex, a mixture of L- and D-lactoylglutathione would result from the GlxI reaction. Obviously, the interaction of the complex with its environment in the protein leads to differences in the flexibility of the glutamate residues. This and the asymmetry of the reaction field in general disables Glu99 from delivering a proton to C2 and Glu172 to transfer a proton to O2.

4. Concluding Remarks

In this paper we have described the structures of the **S**−**E**, **P**−**E**, and intermediate complexes of the reaction of human GlxI, which leads to a qualitative but detailed reaction mechanism for the conversion of the *S*-form of the methylglyoxal thiohemiacetal with glutathione to *S*-D-lactoylglutathione. This mechanism agrees with that proposed on the basis of X-ray structures and other experimental studies on many points, confirming that the zinc center is directly involved in the catalytic process and that the reaction proceeds via an enediolate intermediate. In addition, we have described in detail the process of the substrate binding to the zinc ion. For the *S*-form of the thiohemiacetal, this involves a concurrent process of the substrate entering the active site and displacing zinc-bound water molecules, Glu172 abstracting the proton from C1 and leaving the zinc center, and the formation of the zinc-bound enediolate intermediate. While Glu172 then delivers the proton to C2, Glu99 is responsible for the transfer of the second proton from O1 to O2. For the *R*-thiohemiacetal, the base abstracting the proton from C1 should be Glu99, but to form *S*-D-lactoylglutathione C2 must receive the proton again from Glu172. Therefore, we conclude that the conversion of the two stereoisomers of the thiohemiacetal proceeds via slightly different mechanisms. The stereospecificity of the GlxI reaction results from the effect of the protein environment on the active site zinc complex, which distorts the C_s symmetry of the in vacuo complex and decreases the flexibility of the glutamate residues in such a way that only *S*-D-lactoylglutathione can be formed.

The key element of our approach is the use of effective fragment potentials to represent the electrostatic field generated by the environment of the reaction center. We point out again that our active site model is based on a crystal structure that does not have a transition-state analogue or product bound in the active site. Still, the enzyme is in a catalytically competent conformation to bind the substrate. This suggests that the protein can assume a variety of different reactive conformations, which might be one of the factors that make these enzymes such effective catalysts. Starting from the B-GSH/GlxI crystal structure, we were also able to leverage the active site structure of the HIPC-GSH/GlxI complex by only modifying the model substrate to resemble closely the electronic behavior of the HIPC-GSH inhibitor.

The calculated structures can be of great value in the design of new competitive inhibitors for the enzyme, since they show in detail the interactions of the thiohemiacetal, the *S*-D-lactoylglutathione, and the enediolate intermediate with the active site of glyoxalase I. In principle, the same methodological framework as in this study can be used to probe potential compounds.

Acknowledgment. We thank the Deutsche Forschungsgemeinschaft for financially supporting this project.

JA0105966